Towards Vapour Detection with an Insect Odorant Receptor Bioelectronic Nose

by

Eddyn Oswald Perkins Treacher

A thesis submitted in fulfilment of the
requirements of the degree of
Doctor of Philosophy in Physics
School of Physical and Chemical Sciences
Te Herenga Waka - Victoria University of Wellington

May 2024

Table of contents

Acknowledgements

69450

Rifat, Alex - vapour sensor Erica Cassie - FET sensing setup Rob Keyzers and Jennie Ramirez-Garcia - NMR spectra Patricia Hunt - Computational chemistry

1. Odorant Receptor Biosensors with Carbon Nanotube Network and Graphene Transistors

1.1. Introduction

In **?@sec-thin-film-transistors**, it was established that as carbon nanotubes and graphene are highly sensitive and are easily modified with biomaterials, they make an ideal platform for biosensing [1], [2]. In the early 2000s, it was established that sensitive and selective biosensors could be created by modifying a carbon nanotube field-effect transistor channel with protein receptors [1], [3]. In the following two decades, a wide range of other biological receptors have been attached to carbon nanotube FETs and graphene FETs for the creation of biosensors, including enzymes [4]–[6], antibodies [7]–[9] and aptameric DNA [10]–[12]. These miniaturised 'lab on a chip' devices are of particular interest due to their low cost, rapid use time, simple operation and small size compared with more traditional biological analysis methods [1]. It is hoped that such sensors could be deployed outside the laboratory in a range of front-line settings requiring rapid and reliable detection [13]–[15]. Specific examples include rapid diagnostic testing at a busy medical clinic [16], or the mass detection of biological threats across a large shipment of imported fruit [17], [18].

Rapid developments in this biosensor technology and parallel developments in the understanding of animal olfaction led to these transistors being used in bioelectronic nose applications from the late 2000s onwards [19]–[22]. 'Bioelectronic nose' is a general term dating back to 1961, which refers to the use of an biologically-modified electronic array to detect specific odor traces in a highly selective and sensitive manner. As the name suggests, the signals from this system mimic the electrochemical signals received by olfactory neurons in an animal nose [13], [23], [24]. A biomimetic approach to bioelectronic nose development couples the CNT FET or GFET signal-amplifying transducer element with sensitive components of the animal olfactory system. These components include olfactory cells [25], odorant binding proteins (OBPs) [26], [27] and odorant receptor proteins (olfactory receptors, ORs) [14], [28]. An animal nose can detect volatile odors in the air at low parts-per-trillion concentrations, performance which is far superior to even the best available gas sensor technology. The aim for novel olfactory-based biosensors is to match or surpass this level of accuracy [13], [15], [23].

1.2. Odorant Receptors

1.2.1. *In vivo* Structure and Function

Odorant receptors (ORs) are an essential part of the olfactory systems of most animals, including humans. Vertebrate odorant receptors are part of a group of seven-transmembrane proteins known as G-protein coupled receptors (GPCRs). These transmembrane proteins are terminated with an amine group outside the cell membrane, known as the N-terminus, and terminated with a carboxyl group inside the cell membrane, known as the C-terminus [29]. In an animal nose, odorant receptors are found on the membrane of olfactory cells. Volatile compounds entering the nose selectively bind to specific odorant receptors, which undergo a change in conformation [13], [15]. Some odorant receptors are activated by only a few target compounds, while others respond to many; subtle differences in amino acid composition determine the range of compounds which activate a specific OR [14], [24]. The binding process leads to activation and dissociation of the G-protein within the olfactory cell [30], [31]. Intracellular signalling events triggered by G-protein dissociation are converted to an action potential which is transmitted through neuronal pathways to the brain. The multidimensional combination of receptors activated is then interpreted as a specific odor [13], [15], [23], [30]. ORs let us distinguish between thousands of odors [13]–[15], [30].

1.2.2. Artificial Membranes

Odorant receptors are transmembrane proteins, which are insoluble and tend to aggregate and oligomerise in solution [32]. They therefore require stabilisation from either a specific detergent environment or a membrane layer to preserve their structure and function when solubilised [13], [33]. Odorant receptors can be expressed and isolated using heterologous cell systems, where a host cell replicates a protein from transfected RNA or DNA material [13], [29]. The most commonly used expression cells are human embryonic kidney (HEK) cells [16], [34], *E. Coli* bacteria [14], [35] and *S. cerevisiae* (baker's yeast) [36]. The cell membrane can then be used directly in a sensor [13]. Alternatively, odorant receptors can be embedded in an artificial lipid membrane format that mimics the native cell membrane [32]. These membranes can be produced in large numbers and remain in storage for much longer than live cells [37], [38]. Lipid membranes are constructed from phospholipid molecules, which comprise of a small, hydrophilic, polar 'head' and long, hydrophobic, non-polar 'tail' [39], [40]. These artificial membranes include nanomicelles, nanovesicles (including liposomes), lipid cubic phases, amphipols, and nanodiscs [14], [33]. The small size of these artificial membranes makes them appropriate for use with nanomaterial-based transducers [13], [38].

A nanovesicle is a nanoscopic spherical bilayer fluid sac. There are various types of artificial nanovesicles, including liposomes, ethosomes, transfersomes, niosomes and phytosomes. The type of nanovesicle depends on its chemical makeup [40]. For example, a

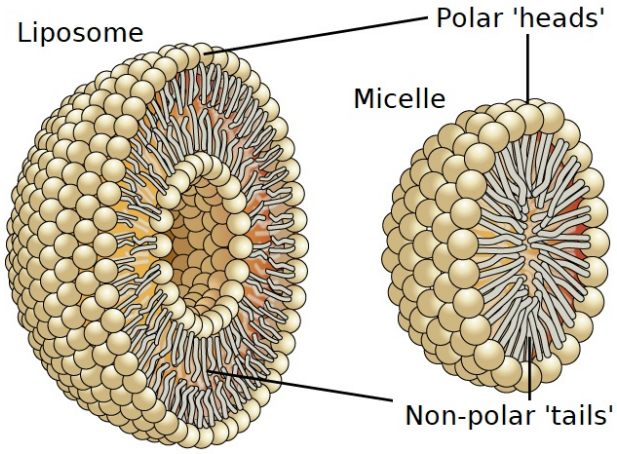

Figure 1.1.: Liposomes and micelles are made up of a lipid membrane, which acts as a substitute for the cell membrane *in vitro*. The polar, hydrophilic 'heads' and non-polar, hydrophobic 'tails' of the component phospholipids are indicated. Adapted from [41].

liposome is made up of phospholipid and cholesterol, and can consist of one or more concentric amphiphilic bilayers. The liposome can contain hydrophobic compounds within the bilayer due to hydrophobic interactions, while hydrophilic compounds are held within the vesicle core or interior [32], [40]. A nanovesicle can be used solely as a format to protect membrane proteins [28], or with the addition of integrated ion channels can mimic the operation of a cell *in vivo*, with intracellular signalling pathways triggered by the membrane proteins [38]. Nanomicelles (or simply micelles) are also nanoscopic and spherical, but unlike nanovesicles have no inner fluid sac [32], [39]. Micelles self-assemble when phospholipid is mixed with detergent. The surface of the micelle is made up of the hydrophilic detergent and phospholipid heads, while the internal core is made up of the hydrophobic phospholipid tail [32]. Hydrophobic compounds can be contained within the core of the micelle [39]. Figure 1.1 illustrates the difference between the liposome and micelle structures.

Nanodiscs have emerged as a model membrane candidate which has many advantages over the more traditional nanovesicle and micelle formats. The nanodisc is a disc-shaped lipid bilayer encompassed by an membrane scaffold protein (MSP) [14], [32], [43]. The amphiphilic membrane scaffold protein protects the exposed, strongly hydrophobic side chains of the nanodisc in an aqueous environment [14], [33]. Unlike liposomes and micelles, there is little variation between the size of individual nanodiscs due to constraints placed on the bilayer by the encompassing scaffold protein used, meaning greater consistency within and between membrane batches [32], [33]. Nanodiscs have also been found to be significantly less prone to non-specific binding (see Section 1.5) than micelles [33]. Another advantage of nanodiscs is that the membrane scaffold protein can be attached to biosensor surfaces at specific affinity tags, for example, the scaffold

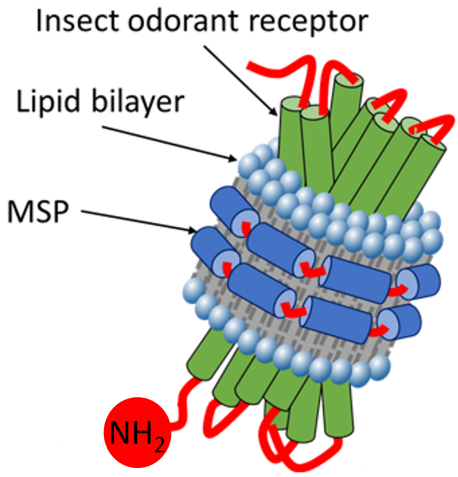

Figure 1.2.: A nanodisc containing an insect odorant receptor transmembrane protein. MSP = membrane scaffold protein, NH_2 = the odorant receptor N-terminus. Reproduced with permission from [42].

protein hexahistidine tag ('his-tag') [33], [43]. Depending on the type of MSP used, a nanodisc measures between 10-20 nm across and can hold either a single or several odorant receptors [32], [43]. The protein coating of the nanodisc makes it particularly stable. The stability of nanodiscs means they can be used to produce particularly reliable and long-lived biosensor devices [14], [37], [44], [45].

1.3. Odorant Receptor Carbon Nanotube and Graphene Biosensors

1.3.1. Sensor Functionalisation

For a bioelectronic nose to operate, sufficient coupling must exist between the bioreceptor element and the sensor transducer. Odorant receptors can be directly attached by physical adsorption; however, this approach is difficult to control, and can result in weak coupling between the odorant receptors and the transducer [13], [23]. Alternatively, a bifunctional linker element may mediate the attachment between functional groups of the bioreceptor and the carbon-ring surface of the transducer in a biochemical process referred to as functionalisation [46]. In this thesis, the amino functional group is of particular interest, but there are many other nucleophilic functional groups available for binding, including carboxyls, hydroxyls, thiols/sulfhydryls, phenols, imidazoles and so on [13], [33]. The linker chemical interacts with the transducer either through stronger covalent bonding or weaker non-covalent bonding. The relative advantages and disadvantages of each type of receptor immobilisation can be found in Table 1.1, while a more

thorough comparison of covalent and non-covalent linker functionalisation can be found in **?@sec-noncovalent-functionalisation**.

Table 1.1.: A comparison of the advantages and disadvantages of different approaches for immobilising odorant receptors onto carbon nanotube or graphene transducers. (Simplicity = the amount of cost, time and effort involved in functionalisation; Stability = the ability for the sensor to operate over a long time and under a range of conditions; Specificity = the ability to attach the receptor in a controlled and directional manner; Strength = the strength of attachment between receptor and transducer; Synergy = the ability for the receptor to attach without negatively impacting transducer operation or restricting receptor activity.)

Attachment Type	Simplicity	Strength	Specificity	Stability	Synergy
Direct Adsorption	High	Low	Low	Low	Medium
Linker, non-covalently tethered	Medium	Medium	Medium	Medium	High
Linker, covalently tethered	Medium	High	High	High	Low

Table 1.2 summarises all published odorant-receptor functionalised carbon nanotube and graphene field-effect transistor-based sensors to date. The majority of published works on this topic come from the Tai Hyun Park group at Seoul National University. The Park group has mainly focused on CNT FETs functionalised with human odorant receptors, but has used a range of different covalent and non-covalent functionalisation techniques when producing the sensors. Three functionalisation methods have been used by both the Park group as well as by a secondary research group: non-covalent glutaraldehyde (GA)-conjugated 1,5-diaminonaphthalene (DAN) functionalisation [23], [24], non-covalent 1-pyrenebutanoic acid N-hydroxysuccinimide ester (PBASE) functionalisation [28], [47], and covalent nickel/nitrilotriacetic acid (Ni-NTA) modified diazonium salt [37], [48]. Interestingly, no single paper compares multiple possible functionalisation techniques directly, making it difficult to assess the quality of various attachment methods. The limit of detection (LOD) could be used as a rough measure of quality. The functionalisation procedure resulting in the lowest limit of detection used was non-covalent [22], though other functionalisation techniques used appear to have more consistent LOD. Furthermore, non-covalent functionalisation of odorant receptors has never been used for vapour sensing. The next section further explores the sensing behaviour of biosensors functionalised following the most commonly-used protocols.

Table 1.2.: Summary of past fabrication methods for odorant receptor-functionalised carbon nanotube and graphene biosensors. PBASE = 1-pyrenebutanoic acid N-hydroxysuccinimide ester, GA = glutaraldehyde, DAN = 1,5-diaminonaphthalene, DMT-MM = 4-(4,6-dimethoxy-1,3,5-triazin-2-yl)-4 methylmorpholinium chloride, NTA = nitrilotriacetic acid, PDL = poly-D-lysine, Ab = Antibody fragments, CNTFET = carbon nanotube field-effect transistor, GFET = graphene field-effect transistor, TX = transfer characteristics.

Attachment	Attachment Method	References	Transducer	OR Type	OR Format	LOD
Non-covalent	Vacuum-drying	Kim, 2009. [49]	CNTFET	Human	Cell membrane	100 fM
	DMT-MM	Yoon, 2009. [19]	CNTFET	Human	Cell membrane	10 fM
	PDL	Jin, 2012. [20]	CNTFET	Human	Nanovesicles	1 fM
		Park, 2012. [50]	CNTFET	Dog	Nanovesicles	1 fM
		Lim, 2014. [16]	CNTFET	Human	Nanovesicles	10 fM
		Lim, 2015. [38]	CNTFET	Human	Nanovesicles	1 fM
		Son, 2015. [51]	CNTFET	Human	Nanovesicles	10 ng/L
		Ahn, 2015. [52]	CNTFET	Human	Nanovesicles	1 fM
	GA-conjugated DAN	Park, 2012. [22]	GFET	Human	Cell membrane	0.04 fM
		Lee, 2012. [21]	CNTFET	Human	Cell membrane	1 fM
		Kwon, 2015. [23]	GFET	Human	Cell membrane	0.1 fM
		Goodwin, 2021. [24]	GFET	Human	Cell membrane	0.5 pM
	PBASE	Murugathas, 2019. [42]	CNTFET	*Insect*	Nanodiscs	1 fM
		Murugathas, 2020. [28]	GFET	*Insect*	Nanovesicles, Nanodiscs	1 fM
		Ahn, 2020. [34]	GFET	Human	Nanovesicles	100 fM
		Yoo, 2022. [47]	CNTFET	Human	Nanomicelles	1 fM
Covalent	Diazonium salt/Ni-NTA	Goldsmith, 2011. [37]	CNTFET	Mouse	Nanomicelles, Nanodiscs	~7 ppb
		Son, 2017. [48]	CNTFET	Human	Nanomicelles	10 fM
	Half-v5 mouse Ab	Lee, 2018. [53]	CNTFET	Human	Nanodiscs	1 fM

1.3.2. Sensing Behaviour

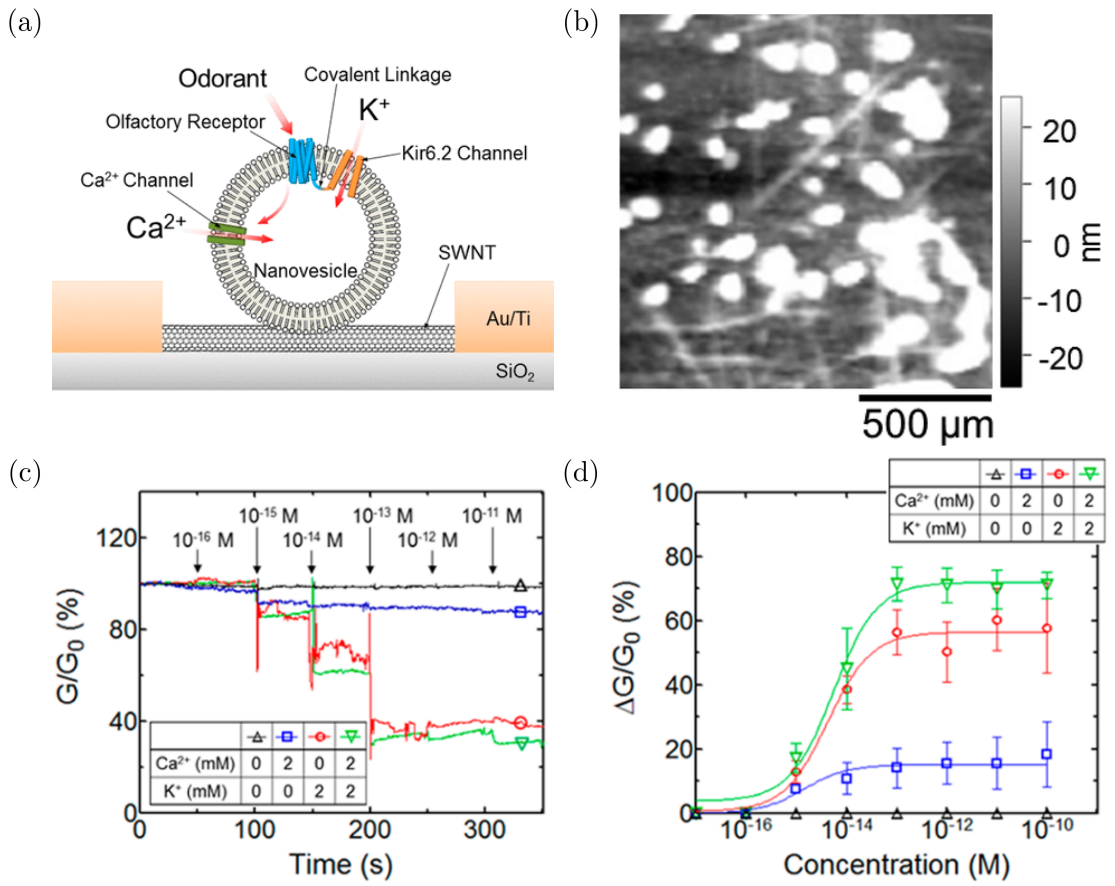

Figure 1.3.: Schematics detailing the nanovesicle-based carbon nanotube field-effect biosensor of Lim *et al.*. (a) shows a schematic of the different elements and signalling pathways present in the sensor, (b) shows an atomic force microscope image of the functionalised device, (c) shows real-time conductance changes resulting from amyl butyrate additions with relevant controls, and (d) shows the dose-dependent response pattern to amyl butyrate. Reproduced with permission from [38].

Nanovesicle-based odorant receptor biosensors can be used to directly mimic the natural behaviour of an odorant receptor, where the presence of analyte leads to a flow of ions into an olfactory cell [13], [38]. Lim *et al.* functionalised a carbon nanotube field-effect transistor with nanovesicles featuring a human odorant receptor hOR2AG1 covalently coupled with a potassium ion channel at the intracellular C-terminus, as well as an endogenous calcium ion channel, as shown in Figure 1.3 (a). These nanovesicles were attached to the random carbon nanotube network through a charge-charge interaction with poly-D-lysine, demonstrated with the atomic force microscope image shown in Figure 1.3 (b). Binding of amyl butyrate to hOR2AG1 causes the OR to change confor-

mation, opening the coupled potassium ion channel and gating the transistor channel. The real-time signal responses associated with amyl butyrate binding are shown by the red trace in Figure 1.3 (c). Intracellular signalling by the odorant receptors means that target binding also opens the calcium ion channel, and responses are therefore seen when just calcium ions are present. However, without potassium or calcium ions present, ion inflow cannot occur and no conductance change occurs. Figure 1.3 (d) shows the relative response size to amyl butyrate with different ions available [38].

Odorant receptors can also be expressed in the native cell membrane and attached directly to the biosensor channel. Here, the changes in odorant receptor conformation that result from analyte binding cause affects the distance between charges on the odorant receptor and the transducer channel, gating the channel [13], [23]. Kwon *et al.* functionalised graphene field-effect transistors with human odorant receptors hOR2AG1 and hOR3A1 using non-covalently attached 1,5-diaminonaphthalene (DAN) modified with glutaraldehyde as a linker, as shown in Figure 1.4 (a). The odorant receptors attach to the GA-modified DAN via a Schiff-base reaction [54]. OR attachment was demonstrated by SEM imaging as well as a significant change in device resistance, shown in Figure 1.4 (b). Both hOR2AG1 and hOR3A1 showed real-time responses to their corresponding target analyte at sub-femtomolar concentrations, as shown in Figure 1.4 (c) and Figure 1.4 (d) respectively. No responses were seen from linker-modified graphene to similar analyte concentrations. The dose-dependent response curve of both these odorant receptor sensors is shown in Figure 1.4 (e). As in Figure 1.3 (d), a Langmuir-type dose response behaviour was seen, where a logarithmic increase in signal response is observed for sub-femtomolar or femtomolar concentration analyte additions, which gives way to saturation behaviour with picomolar additions.

Vapour Environment

Goldsmith *et al.* have previously demonstrated it is possible to specifically detect eugenol vapour using a single-CNT device functionalised with mOR174-9 odorant receptors in either a surfactant (digitonin) or nanodisc format. In the first study of this kind, the mOR CNT FETs were exposed to nitrogen flow at 50% relative humidity. The resistance across a device gated at $V_g = 0$ V was measured while a specific concentration of the positive ligand eugenol was added to the constant flow for 100 s, then removed from the flow for 100 s. This cycle was repeated five times. Figure 1.5 (a) shows that significant real-time current increases of up to $\sim 9\%$ were observed during each cycle of exposure to eugenol. The device still responded to eugenol cycles after 69 days of storage in 25% (v/v) ethanol at 4°C. This nicely-behaved and persistent activity may result from the long-lived nanodisc format used [37]. As far as the author knows, there has been no investigation up until now into whether this behaviour can be replicated for insect odorant receptor devices. It is not clear that iORs can simply be substituted for mORs for vapour sensing. The reasons for this distinction are made in the subsequent section.

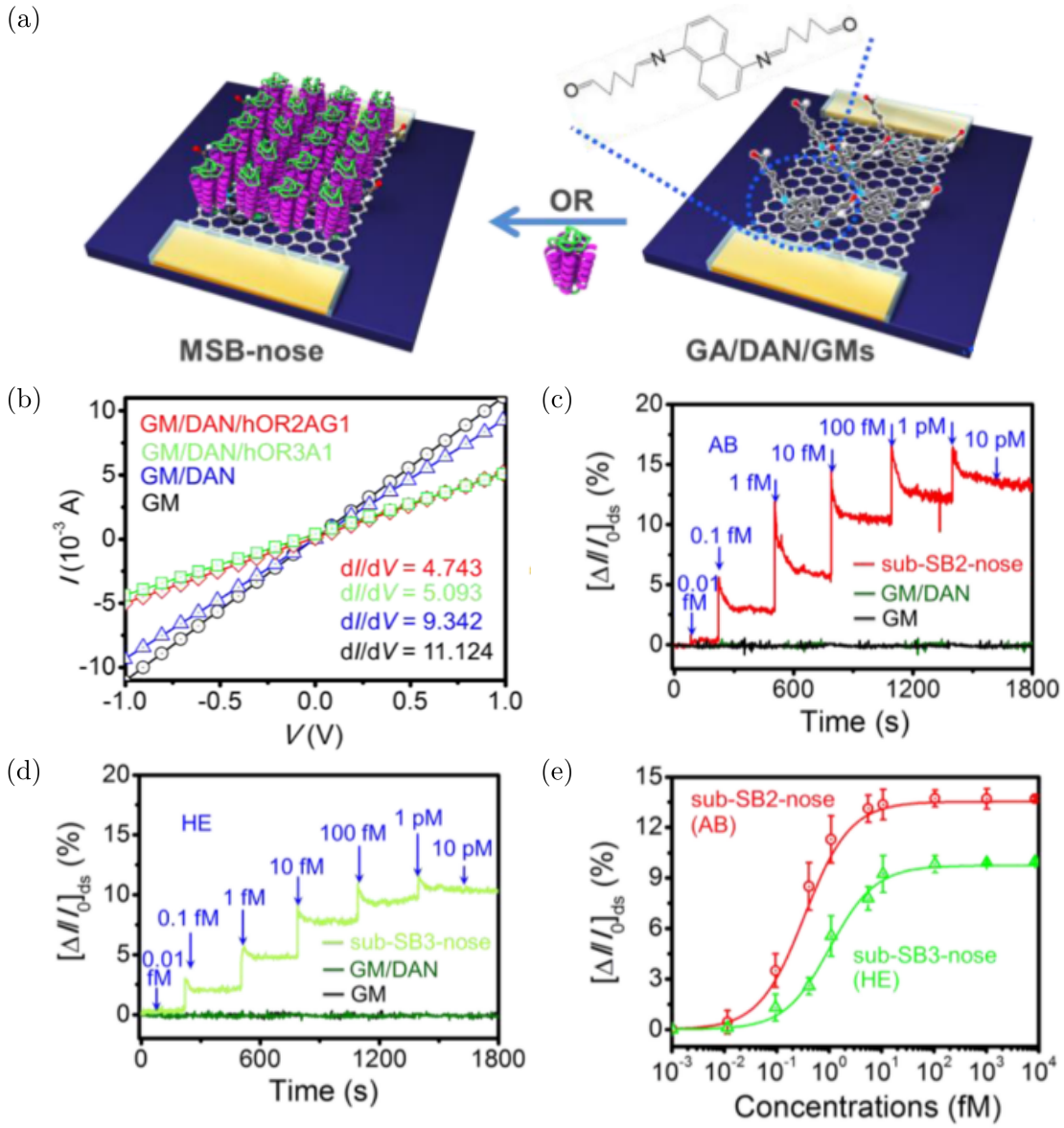

Figure 1.4.: Schematics showing the odorant receptor-functionalised graphene field-effect biosensor of Kwon *et al.*. (a) shows the functionalisation of odorant receptors onto graphene using non-covalently attached GA-modified DAN linker; (b) compares transfer characteristics of the device with graphene only (GM), graphene with DAN linker (GM/DAN), and after modification with one of two different ORs (hOR2AG1, hOR3A1); (c) shows the real-time responses of the hOR2AG1-modified transistor (sub-SB2) to various concentrations of amyl butyrate (AB) analyte; (d) shows the real-time responses of the hOR3A1-modified transistor (sub-SB3) to various concentrations of helional (HE) analyte; and (e) shows the dose-dependent response curve corresponding to the sub-SB2 and sub-SB3 sensors. Reproduced with permission from [23].

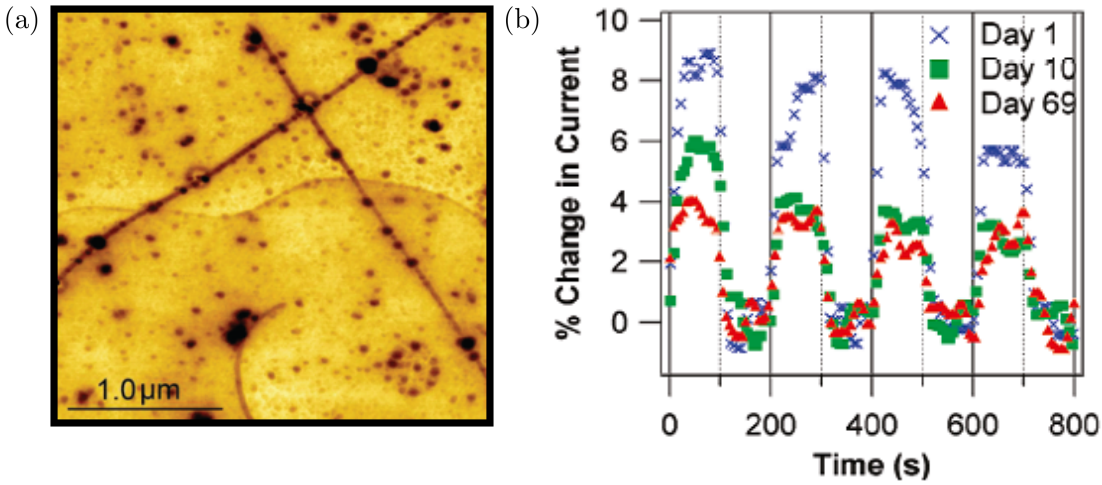

Figure 1.5.: The functionalisation of mOR174-9 nanodiscs onto single-CNT field effect transistor vapour sensing use is demonstrated with an atomic force microscope image in (a), while (b) shows real-time responses of the sensor to 2 ppm eugenol vapour. The response to eugenol on day 69 (red triangles) indicates that the device retains the ability to respond to eugenol 10 weeks after functionalisation. Reproduced with permission from [37].

1.4. Insect Odorant Receptor Biosensors

1.4.1. *In Vivo* Structure and Function

Insect odorant (or olfactory) receptors (iORs) are a diverse range of odorant-sensitive transmembrane proteins located in dendrite cells of sensory hairs, known as sensilla, on the antennae and maxillary palps of an insect [57], [58]. Insects possess a specific set of iORs tailored towards their ecological role (iORx, where the "x" denotes the OR variant), as well as a co-receptor known as "ORCO" (Odorant Receptor Co-Receptor). In the insect, a given iORx is activated by volatile compounds, while the ORCO co-receptor is insensitive to VOCs but couples with iORx to form a heteromeric complex, which activates intracellular signalling via its ion channel activity. *In vivo*, the complex is required for VOC detection and operates as a non-selective cation channel. This channel opens to allow ions to travel across the cell membrane in response to iOR interaction with VOCs [45], [55], [58]–[62].

iORs were initially thought to be similar in structure to vertebrate odorant receptors, but is now known that iORs have a completely different topology and mechanism to GPCRs, despite also possessing seven-transmembrane domains. Their configuration in the membrane is inverted. Equivalently, the carboxyl group or 'C terminus' of the iOR sits outside the membrane of a cell, and the amine group or 'N terminus' of the iOR

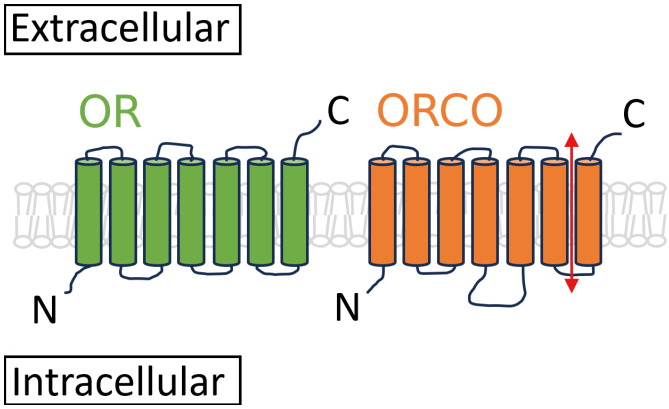

Figure 1.6.: The tuning OR and odorant receptor coreceptor (ORCO) on the native cell membrane, with C-terminus and N-terminus indicated. The red arrow indicates the location of ion transport across the membrane. Adapted from [55], [56].

sits inside the cell membrane [29], [61], [62]. The *in vivo* configuration of the odorant receptor on the cell membrane is illustrated in Figure 1.6.

Each odorant receptor of the *Drosophilia melanogaster* sensilla will respond to a variety of odor compound. Odors which provoke a particularly strong response from a specific odorant receptor are referred to in the literature as 'positive ligands' for that receptor [28], [42]. The strength of response by a specific OR depends on the compound being detected; furthermore, there may be no response to a compound, or one compound may inhibit the response of the receptor to other compounds. Odor compounds which provoke no response from a particular receptor are referred to as 'negative ligands' for that receptor [28], [42]. A comprehensive database that details the various *Drosophilia melanogaster* odorant receptors and their response profile to a range of volatile compounds can be consulted online [63].

1.4.2. Sensing Behaviour

As in the case of vertebrate ORs, recent studies have shown that iORs each interact with a specific VOC or a specific range of VOCs and can also be used in bioelectronic nose applications. However, the sensing mechanisms underlying their use *in vitro* are not currently well-understood [28], [42], [64]. From further development and examination of iOR-based biosensors, new insights into the mechanisms at play may emerge. Previously, the literature has primarily focused on the operation of iOR-FET biosensors in an aqueous environment. Here, carbon nanotube or graphene FETs have been non-covalently functionalised with insect odorant receptors in either a nanodisc or liposome format. The high surface-to-volume ratio of carbon nanotubes and graphene allow for the odorant

receptors to be densely immobilised across the channel surface. The functionalised channel is placed in a liquid-gated environment contained in polydimethylsiloxane (PDMS) and gated with a Ag-AgCl reference electrode (see **?@sec-gating**). Phosphate buffered saline (PBS) is used as the liquid gate electrolyte [28], [42]. A small amount of DMSO is also added to the electrolyte, a dipolar solvent which is widely used to solubilise poorly soluble analytes in a biological setting [65].

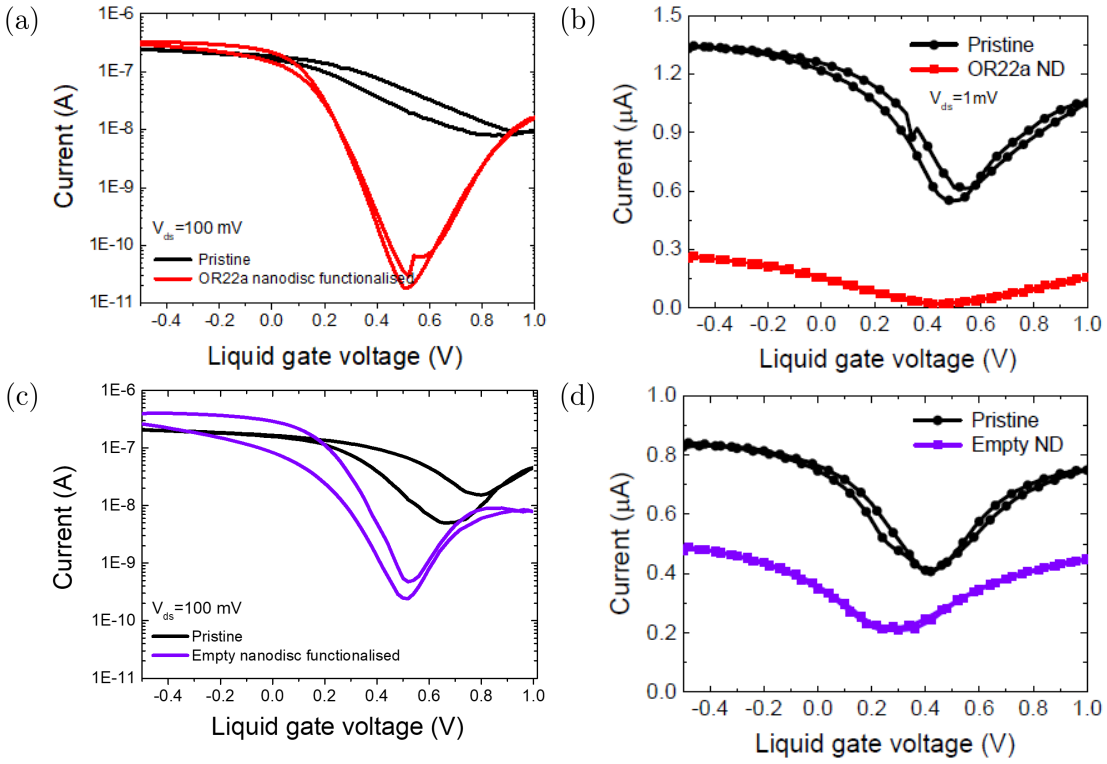

Figure 1.7.: Transfer characteristic curves before and after functionalisation of (a) an OR22a nanodisc-functionalised CNT network FET, (b) an OR22a nanodisc-functionalised graphene FET, (c) an empty nanodisc-functionalised CNT network FET and (d) an empty nanodisc-functionalised graphene FET. Reproduced with permission from [28], [42].

Functionalisation of a FET device channel with iORs significantly alters the transfer characteristics of that channel. Murugathas *et al.* found that successful functionalisation of a CNTFET device with iORs would typically increase the device on-current, increase its on-off ratio and cause a significant negative shift in threshold voltage, as shown in Figure 1.7 (a) [42]. Meanwhile, successful functionalisation of a graphene device with iORs would typically dramatically decrease the device on-current and cause a negative shift in Dirac voltage, as seen in Figure 1.7 (b) [28]. These changes are not simply the result of linker attachment to the channel surface [42]. It is thought that the negative shift of both threshold and Dirac voltages are caused by the N-terminus amine groups

on the odorant receptors or amine groups on the nanodisc membrane scaffold proteins donating electrons to the device channel, which has a similar effect to doping the channel with impurities [28], [42], [66]. Note that very similar changes occur when functionalising with empty nanodiscs which contain no odorant receptors, shown in Figure 1.7 (c) and Figure 1.7 (d). Unless the odorant receptors attach preferentially to the network over nanodiscs, it appears the gating effect is predominantly due to the large-scale attachment of nanodisc membranes.

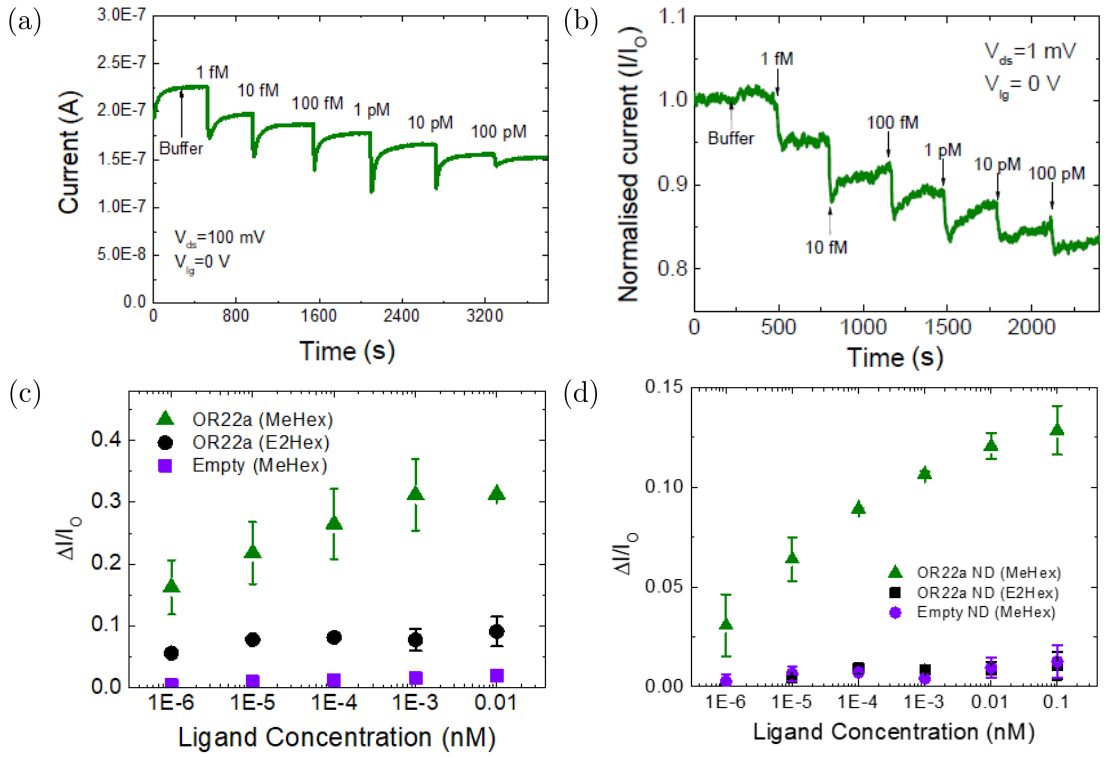

Figure 1.8.: Real-time responses to concentrations of methyl hexanoate in 1× phosphate buffer saline (PBS) with 1% v/v DMSO by (a) an OR22a nanodisc-functionalised CNT network FET and (b) an OR22a nanodisc-functionalised graphene FET, alongside the normalised signal response curves corresponding to (c) CNT network FETs and (d) graphene FETs. The response curves show the cumulative responses of OR22a-functionalised devices to both the positive ligand methyl hexanoate (green) and negative ligand *trans*-2-hexan-1-al (black). They also show the cumulative response of a empty nanodisc functionalised device to methyl hexanoate (purple). Reproduced with permission from [28], [42].

Interactions between iORs attached to the channel, such as OR22a, and positive ligands added to the electrolyte environment, such as methyl hexanoate (MeHex), can alter the current flowing through the channel. These current changes can be monitored over time

and interpreted as real-time sensor responses. Figure 1.8 (a) and (b) show the respective responses of the OR22a-functionalised CNT FET and graphene FET in Figure 1.7 to methyl hexanoate in real-time. This result demonstrates that iOR-FETs are sensitive down to the femtomolar scale in an aqueous environment. Figure 1.8 (c) and (d) compare the average methyl hexanoate responses of multiple devices to that of relevant controls. It was verified that the OR22a-functionalised devices would not respond to *trans*-2-hexan-1-al, the negative ligand for OR22a; it was also verified that empty nanodiscs would not respond non-selectively to the positive ligand [28], [42].

The reduction in the channel current of a functionalised FET upon exposure to a positive ligand is notably different to the signal transduction mechanism of iORs *in vivo*, since ORCO does not appear to be required for an iOR bioelectronic nose to function. It has been proposed that the signal response results from the positive ligand binding to the iOR protein, causing it to change shape. Cheema *et al.* used neutron reflectometry to demonstrate that OR22a nanodiscs undergo a 1 nm height change after ethyl hexanoate exposure, likely resulting from a structural change [45]. This change most likely affects the channel in one of two ways. The first involves transfer of charge from the iOR to the channel, reducing I_d and causing a negative threshold voltage (or Dirac point) shift. Another could be a more indirect electrostatic gating effect, due to the movement of charge within the Debye screening length of the channel. The Debye length of 1× PBS buffer is typically much shorter than the height of a single nanodisc [42]. However, if structural changes in the iOR were primarily occurring at its base, it is still possible that the electrostatic gating could be the primary sensing mechanism.

1.5. Non-Specific Binding

Non-specific binding (NSB) refers to any attachment to the sensor channel not related to the specific analyte of interest which could interfere with sensing. Liquid-gated graphene and carbon nanotube devices are highly sensitive to the approach of charge within the Debye length of the device channel [67]. Non-specific adsorption of the analyte or ambient contamination from numerous elements used in fabricating the biosensor can lead to signal responses not attributable to the mechanism of interest (see **?@sec-CNT-sensing-mechanisms**), leading to false positives when sensing [33], [46], [67], [68]. Non-specific adsorption can occur on the channel as well as the the source-drain and gate electrodes [68]. A variety of measures can be taken to prevent NSB from occurring. Once bioreceptors have been attached to the channel, remaining exposed carbon nanotubes can be passivated with chemical coatings such as Tween-20 [68], PEG [21], [46], and ethanolamine [10], [69]. If measuring multiple channels in a multiplexed array, one channel can be left uncoated to compare the sensing response in a process known as 'internal referencing' [67].

Non-specific binding is particularly significant for protein-functionalised devices. Proteins may be spontaneously adsorbed onto carbon nanotube or graphene surfaces during

functionalisation in a manner which is not linker-mediated [46], [66], [68]. Non-covalently bound proteins may also detach and reattach to available surfaces in a non-specific manner when exposed to a high ionic strength electrolyte post-functionalisation [13]. Such adsorption is known to reduce the conductance of device channels containing semiconducting carbon nanotubes, which may result from electron transfer between amino acid residues and the nanotube network. The significance of this effect is increased when electrodes are not sufficiently passivated or encapsulated due to modulation of the Schottky barrier at the metal-carbon nanotube interface [68].

A. Vapour System Hardware

Table A.1.: Major components used in construction of the vapour delivery system described in this thesis.

Description	Part No.	Manufacturer
Mass flow controller, 20 sccm full scale	GE50A013201SBV020	MKS Instruments
Mass flow controller, 200 sccm full scale	GE50A013202SBV020	MKS Instruments
Mass flow controller, 500 sccm full scale	FC-2901V	Tylan
Analogue flowmeter, 240 sccm max. flow	116261-30	Dwyer
Micro diaphragm pump	P200-B3C5V-35000	Xavitech
Analogue flow controller, for micro diaphragm pump	X3000450	Xavitech
10 mL Schott bottle	218010802	Duran
PTFE connection cap system	Z742273	Duran
Baseline VOC-TRAQ flow cell, red	043-951	Mocon
Humidity and temperature sensor	T9602	Telaire
Enclosure, for humidity and temperature sensor	MC001189	Multicomp Pro

B. Python Code for Data Analysis

B.1. Code Repository

The code used for general analysis of field-effect transistor devices in this thesis was written with Python 3.8.8. Contributors to the code used include Erica Cassie, Erica Happe, Marissa Dierkes and Leo Browning. The code is located on GitHub and the research group OneDrive, and is available on request.

B.2. Atomic Force Microscope Histogram Analysis

The purpose of this code is to analyse atomic force microscope (AFM) images of carbon nanotube networks in .xyz format taken using an atomic force microscope and processed in Gwyddion (see **?@sec-afm-characterisation**). It was originally designed by Erica Happe in Matlab, and adapted by Marissa Dierkes and myself for use in Python. The code imports the .xyz data and sorts it into bins 0.15 nm in size for processing. To perform skew-normal distribution fits, both *scipy.optimize.curve_fit* and *scipy.stats.skewnorm* modules are used in this code.

B.3. Raman Spectroscopy Analysis

The purpose of this code is to analyse a series of Raman spectra taken at different points on a single film (see **?@sec-raman-characterisation**). Data is imported in a series of tab-delimited text files, with the low wavenumber spectrum ($100\ \mathrm{cm}^{-1} - 650\ \mathrm{cm}^{-1}$) and high wavenumber spectrum ($1300\ \mathrm{cm}^{-1} - 1650\ \mathrm{cm}^{-1}$) imported in separate datafiles for each scan location.

B.4. Field-Effect Transistor Analysis

The purpose of this code is to analyse electrical measurements taken of field-effect transistor (FET) devices. Electrical measurements were either taken from the Keysight 4156C Semiconductor Parameter Analyser, National Instruments NI-PXIe or Keysight B1500A Semiconductor Device Analyser as discussed in **?@sec-electrical-characterisation**;

the code is able to analyse data in .csv format taken from all three measurement setups. The main Python file in the code base consists of three related but independent modules: the first analyses and plots sensing data from the FET devices, the second analyses and plots transfer characteristics from channels across a device, and the third compares individual channel characteristics before and after a modification or after each of several modifications. The code base also features a separate config file and style sheet which govern the behaviour of the main code. The code base was designed collaboratively by myself and Erica Cassie over GitHub using the Sourcetree Git GUI.

Bibliography

[1] Douglas R. Kauffman and Alexander Star. "Electronically monitoring biological interactions with carbon nanotube field-effect transistors". In: *Chemical Society Reviews* 37.6 (May 2008), pp. 1197–1206. ISSN: 1460-4744. DOI: 10.1039/B709567H. URL: https://pubs.rsc.org/en/content/articlehtml/2008/cs/b709567h%20https://pubs.rsc.org/en/content/articlelanding/2008/cs/b709567h.

[2] Yasuhide Ohno, Kenzo Maehashi, and Kazuhiko Matsumoto. "Label-free biosensors based on aptamer-modified graphene field-effect transistors". In: *Journal of the American Chemical Society* 132.51 (Dec. 2010), pp. 18012–18013. ISSN: 00027863. DOI: 10.1021/ja108127r. URL: https://pubs.acs.org/doi/full/10.1021/ja108127r.

[3] Robert J. Chen, Sarunya Bangsaruntip, Katerina A. Drouvalakis, et al. "Noncovalent functionalization of carbon nanotubes for highly specific electronic biosensors". In: *Proceedings of the National Academy of Sciences of the United States of America* 100.9 (Apr. 2003), p. 4984. ISSN: 00278424. DOI: 10.1073/PNAS.0837064100. URL: /pmc/articles/PMC154284/%20/pmc/articles/PMC154284/?report=abstract%20https://www.ncbi.nlm.nih.gov/pmc/articles/PMC154284/.

[4] G. J. Lee, J. E. Lim, J. H. Park, et al. "Neurotransmitter detection by enzyme-immobilized CNT-FET". In: *Current Applied Physics* 9.1 (Jan. 2009), S25–S28. ISSN: 1567-1739. DOI: 10.1016/J.CAP.2008.08.031.

[5] Meng Zhang, Caizhi Liao, Chun Hin Mak, et al. "Highly sensitive glucose sensors based on enzyme-modified whole-graphene solution-gated transistors". In: *Scientific Reports 2015 5:1* 5.1 (Feb. 2015), pp. 1–6. ISSN: 2045-2322. DOI: 10.1038/srep08311. URL: https://www.nature.com/articles/srep08311.

[6] Alexandra Dudina, Urs Frey, and Andreas Hierlemann. "Carbon-Nanotube-Based Monolithic CMOS Platform for Electrochemical Detection of Neurotransmitter Glutamate". In: *Sensors 2019, Vol. 19, Page 3080* 19.14 (July 2019), p. 3080. ISSN: 1424-8220. DOI: 10.3390/S19143080. URL: https://www.mdpi.com/1424-8220/19/14/3080/htm%20https://www.mdpi.com/1424-8220/19/14/3080.

[7] Jun Pyo Kim, Byung Yang Lee, Seunghun Hong, et al. "Ultrasensitive carbon nanotube-based biosensors using antibody-binding fragments". In: *Analytical biochemistry* 381.2 (Oct. 2008), pp. 193–198. ISSN: 1096-0309. DOI: 10.1016/J.AB.2008.06.040. URL: https://pubmed.ncbi.nlm.nih.gov/18640089/.

[8] Joon Hyung Jin, Junhyup Kim, Taejin Jeon, et al. "Real-time selective monitoring of allergenic Aspergillus molds using pentameric antibody-immobilized single-walled carbon nanotube-field effect transistors". In: *RSC Advances* 5.20 (Jan. 2015), pp. 15728–15735. ISSN: 2046-2069. DOI: 10.1039/C4RA15815F. URL: https://pubs.rsc.org/en/content/articlehtml/2015/ra/c4ra15815f%20https://pubs.rsc.org/en/content/articlelanding/2015/ra/c4ra15815f.

[9] Deana Kwong Hong Tsang, Tyler J. Lieberthal, Clare Watts, et al. "Chemically Functionalised Graphene FET Biosensor for the Label-free Sensing of Exosomes". In: *Scientific Reports* 9.1 (Sept. 2019), pp. 1–10. ISSN: 20452322. DOI: 10.1038/s41598-019-50412-9. URL: https://www.nature.com/articles/s41598-019-50412-9.

[10] Kenzo Maehashi, Taiji Katsura, Kagan Kerman, et al. "Label-free protein biosensor based on aptamer-modified carbon nanotube field-effect transistors". In: *Analytical Chemistry* 79.2 (Jan. 2007), pp. 782–787. ISSN: 00032700. DOI: 10.1021/ac060830g. URL: https://pubs.acs.org/doi/full/10.1021/ac060830g.

[11] Ning Gao, Teng Gao, Xiao Yang, et al. "Specific detection of biomolecules in physiological solutions using graphene transistor biosensors". In: *Proceedings of the National Academy of Sciences of the United States of America* 113.51 (Dec. 2016), pp. 14633–14638. ISSN: 10916490. DOI: 10.1073/PNAS.1625010114/SUPPL_FILE/PNAS.201625010SI.PDF. URL: https://www.pnas.org/doi/abs/10.1073/pnas.1625010114.

[12] Hong Phan T. Nguyen, Thanihaichelvan Murugathas, and Natalie O.V. Plank. "Comparison of Duplex and Quadruplex Folding Structure Adenosine Aptamers for Carbon Nanotube Field Effect Transistor Aptasensors". In: *Nanomaterials (Basel, Switzerland)* 11.9 (Sept. 2021). ISSN: 2079-4991. DOI: 10.3390/NANO11092280. URL: https://pubmed.ncbi.nlm.nih.gov/34578596/.

[13] Tran Thi Dung, Yunkwang Oh, Seon Jin Choi, et al. "Applications and Advances in Bioelectronic Noses for Odour Sensing". In: *Sensors 2018, Vol. 18, Page 103* 18.1 (Jan. 2018), p. 103. ISSN: 1424-8220. DOI: 10.3390/S18010103. URL: https://www.mdpi.com/1424-8220/18/1/103/htm%20https://www.mdpi.com/1424-8220/18/1/103.

[14] Heehong Yang, Minju Lee, Daesan Kim, et al. "Bioelectronic Nose Using Olfactory Receptor-Embedded Nanodiscs". In: *Methods in molecular biology (Clifton, N.J.)* 1820 (2018), pp. 239–249. ISSN: 1940-6029. DOI: 10.1007/978-1-4939-8609-5_18. URL: https://pubmed.ncbi.nlm.nih.gov/29884950/.

[15] Chuntae Kim, Kyung Kwan Lee, Moon Sung Kang, et al. "Artificial olfactory sensor technology that mimics the olfactory mechanism: a comprehensive review". In: *Biomaterials Research 2022 26:1* 26.1 (Aug. 2022), pp. 1–13. ISSN: 2055-7124. DOI: 10.1186/S40824-022-00287-1. URL: https://biomaterialsres.biomedcentral.com/articles/10.1186/s40824-022-00287-1.

[16] Jong Hyun Lim, Juhun Park, Eun Hae Oh, et al. "Nanovesicle-based bioelectronic nose for the diagnosis of lung cancer from human blood". In: *Advanced healthcare materials* 3.3 (2014), pp. 360–366. ISSN: 2192-2659. DOI: 10.1002/ADHM.201300174. URL: https://pubmed.ncbi.nlm.nih.gov/23868879/.

[17] *About - B3 | Science Solutions for Better Border Biosecurity*. URL: https://www.b3nz.org.nz/about/ (visited on 2024-05-17).

[18] *Queensland fruit fly | NZ Government*. URL: https://www.mpi.govt.nz/biosecurity/pests-and-diseases-not-in-new-zealand/horticultural-pests-and-diseases-not-in-nz/queensland-fruit-fly/ (visited on 2024-05-17).

[19] Wyeonseok Yoon, Sang Hun Lee, Oh Seok Kwon, et al. "Polypyrrole nanotubes conjugated with human olfactory receptors: high-performance transducers for FET-type bioelectronic noses". In: *Angewandte Chemie (International ed. in English)* 48.15 (Mar. 2009), pp. 2755–2758. ISSN: 1521-3773. DOI: 10.1002/ANIE.200805171. URL: https://pubmed.ncbi.nlm.nih.gov/19274689/.

[20] Hye Jun Jin, Sang Hun Lee, Tae Hyun Kim, et al. "Nanovesicle-based bioelectronic nose platform mimicking human olfactory signal transduction". In: *Biosensors and Bioelectronics* 35.1 (May 2012), pp. 335–341. ISSN: 09565663. DOI: 10.1016/j.bios.2012.03.012. URL: https://pubmed.ncbi.nlm.nih.gov/22475887/.

[21] Sang Hun Lee, Hye Jun Jin, Hyun Seok Song, et al. "Bioelectronic nose with high sensitivity and selectivity using chemically functionalized carbon nanotube combined with human olfactory receptor". In: *Journal of biotechnology* 157.4 (Feb. 2012), pp. 467–472. ISSN: 1873-4863. DOI: 10.1016/J.JBIOTEC.2011.09.011. URL: https://pubmed.ncbi.nlm.nih.gov/21945089/.

[22] Seon Joo Park, Oh Seok Kwon, Sang Hun Lee, et al. "Ultrasensitive flexible graphene based field-effect transistor (FET)-type bioelectronic nose". In: *Nano Letters* 12.10 (Oct. 2012), pp. 5082–5090. ISSN: 15306984. DOI: 10.1021/NL301714X/SUPPL_FILE/NL301714X_SI_001.PDF. URL: https://pubs.acs.org/doi/full/10.1021/nl301714x.

[23] Oh Seok Kwon, Hyun Seok Song, Seon Joo Park, et al. "An Ultrasensitive, Selective, Multiplexed Superbioelectronic Nose That Mimics the Human Sense of Smell". In: *Nano Letters* 15.10 (Oct. 2015), pp. 6559–6567. ISSN: 15306992. DOI: 10.1021/acs.nanolett.5b02286. URL: https://pubs.acs.org/doi/full/10.1021/acs.nanolett.5b02286.

[24] Danielle M. Goodwin, Ffion Walters, Muhammad Munem Ali, et al. "Graphene bioelectronic nose for the detection of odorants with human olfactory receptor 2ag1". In: *Chemosensors* 9.7 (July 2021), p. 174. ISSN: 22279040. DOI: 10.3390/CHEMOSENSORS9070174/S1. URL: https://www.mdpi.com/2227-9040/9/7/174/htm%20https://www.mdpi.com/2227-9040/9/7/174.

[25] Ping Wang, Qingjun Liu, Ying Xu, et al. "Olfactory and taste cell sensor and its applications in biomedicine". In: *Sensors and Actuators A: Physical* 139.1-2 (Sept. 2007), pp. 131–138. ISSN: 0924-4247. DOI: 10.1016/J.SNA.2007.05.018.

[26] Melanie Larisika, Caroline Kotlowski, Christoph Steininger, et al. "Electronic Olfactory Sensor Based on A. mellifera Odorant-Binding Protein 14 on a Reduced Graphene Oxide Field-Effect Transistor". In: *Angewandte Chemie (International ed. in English)* 54.45 (Nov. 2015), pp. 13245–13248. ISSN: 1521-3773. DOI: 10.1002/ANIE.201505712. URL: https://pubmed.ncbi.nlm.nih.gov/26364873/.

[27] Caroline Kotlowski, Melanie Larisika, Patrick M. Guerin, et al. "Fine discrimination of volatile compounds by graphene-immobilized odorant-binding proteins". In: *Sensors and Actuators, B: Chemical* 256 (Mar. 2018), pp. 564–572. ISSN: 09254005. DOI: 10.1016/J.SNB.2017.10.093.

[28] Thanihaichelvan Murugathas, Cyril Hamiaux, Damon Colbert, et al. "Evaluating insect odorant receptor display formats for biosensing using graphene field effect transistors". In: *ACS Applied Electronic Materials* 2.11 (Nov. 2020), pp. 3610–3617. ISSN: 26376113. DOI: 10.1021/ACSAELM.0C00677. URL: https://pubs.acs.org/doi/full/10.1021/acsaelm.0c00677.

[29] Richard Glatz and Kelly Bailey-Hill. "Mimicking nature's noses: From receptor deorphaning to olfactory biosensing". In: *Progress in Neurobiology* 93.2 (Feb. 2011), pp. 270–296. ISSN: 0301-0082. DOI: 10.1016/J.PNEUROBIO.2010.11.004.

[30] Linda Buck and Richard Axel. "A novel multigene family may encode odorant receptors: A molecular basis for odor recognition". In: *Cell* 65.1 (Apr. 1991), pp. 175–187. ISSN: 0092-8674. DOI: 10.1016/0092-8674(91)90418-X.

[31] Meng Zhang, Miao Gui, Zi Fu Wang, et al. "Cryo-EM structure of an activated GPCR–G protein complex in lipid nanodiscs". In: *Nature Structural and Molecular Biology* 28.3 (Mar. 2021), pp. 258–267. ISSN: 15459985. DOI: 10.1038/S41594-020-00554-6.

[32] Abhinav Nath, William M. Atkins, and Stephen G. Sligar. "Applications of phospholipid bilayer nanodiscs in the study of membranes and membrane proteins". In: *Biochemistry* 46.8 (Feb. 2007), pp. 2059–2069. ISSN: 00062960. DOI: 10.1021/BI602371N. URL: https://pubs.acs.org/doi/full/10.1021/bi602371n.

[33] Virginie Früh, Ad P. Ijzerman, and Gregg Siegal. "How to catch a membrane protein in action: A review of functional membrane protein immobilization strategies and their applications". In: *Chemical Reviews* 111.2 (Feb. 2011), pp. 640–656. ISSN: 00092665. DOI: 10.1021/CR900088S/ASSET/IMAGES/MEDIUM/CR-2009-00088S_0002.GIF. URL: https://pubs.acs.org/doi/full/10.1021/cr900088s.

[34] Sae Ryun Ahn, Ji Hyun An, Seung Hwan Lee, et al. "Peptide hormone sensors using human hormone receptor-carrying nanovesicles and graphene FETs". In: *Scientific reports* 10.1 (Dec. 2020). ISSN: 2045-2322. DOI: 10.1038/S41598-019-57339-1. URL: https://pubmed.ncbi.nlm.nih.gov/31942024/.

[35] Heehong Yang, Daesan Kim, Jeongsu Kim, et al. "Nanodisc-Based Bioelectronic Nose Using Olfactory Receptor Produced in Escherichia coli for the Assessment of the Death-Associated Odor Cadaverine". In: *ACS Nano* 11.12 (Dec. 2017), pp. 11847–11855. ISSN: 1936086X. DOI: 10.1021/ACSNANO.7B04992/ASSET/IMAGES/NN-2017-04992T_M003.GIF. URL: https://pubs.acs.org/doi/full/10.1021/acsnano.7b04992.

[36] Jonathan D. Bohbot and Sefi Vernick. "The Emergence of Insect Odorant Receptor-Based Biosensors". In: *Biosensors 2020, Vol. 10, Page 26* 10.3 (Mar. 2020), p. 26. ISSN: 2079-6374. DOI: 10.3390/BIOS10030026. URL: https://www.mdpi.com/2079-6374/10/3/26/htm%20https://www.mdpi.com/2079-6374/10/3/26.

[37] Brett R. Goldsmith, Joseph J. Mitala, Jesusa Josue, et al. "Biomimetic chemical sensors using nanoelectronic readout of olfactory receptor proteins". In: *ACS Nano* 5.7 (July 2011), pp. 5408–5416. ISSN: 19360851. DOI: 10.1021/NN200489J/SUPPL_FILE/NN200489J_SI_001.PDF. URL: https://pubs.acs.org/doi/full/10.1021/nn200489j.

[38] Jong Hyun Lim, Eun Hae Oh, Juhun Park, et al. "Ion-channel-coupled receptor-based platform for a real-time measurement of G-protein-coupled receptor activities". In: *ACS nano* 9.2 (Feb. 2015), pp. 1699–1706. ISSN: 1936-086X. DOI: 10.1021/NN506494E. URL: https://pubmed.ncbi.nlm.nih.gov/25625737/.

[39] Anamika Bose, Debanwita Roy Burman, Bismayan Sikdar, et al. "Nanomicelles: Types, properties and applications in drug delivery". In: *IET Nanobiotechnology* 15.1 (Feb. 2021), p. 19. ISSN: 17518741. DOI: 10.1049/NBT2.12018. URL: /pmc/articles/PMC8675821/%20/pmc/articles/PMC8675821/?report=abstract%20https://www.ncbi.nlm.nih.gov/pmc/articles/PMC8675821/.

[40] Delly Ramadon, Maeliosa T.C. McCrudden, Aaron J. Courtenay, et al. "Enhancement strategies for transdermal drug delivery systems: current trends and applications". In: *Drug delivery and translational research* 12.4 (Apr. 2022), pp. 758–791. ISSN: 2190-3948. DOI: 10.1007/S13346-021-00909-6. URL: https://pubmed.ncbi.nlm.nih.gov/33474709/.

[41] CNX OpenStax. *File:OSC Microbio 07 03 micelle.jpg*. 2016. URL: https://commons.wikimedia.org/wiki/File:OSC_Microbio_07_03_micelle.jpg%20https://creativecommons.org/licenses/by/4.0/legalcode (visited on 2024-04-29).

[42] Thanihaichelvan Murugathas, Han Yue Zheng, Damon Colbert, et al. "Biosensing with Insect Odorant Receptor Nanodiscs and Carbon Nanotube Field-Effect Transistors". In: *ACS Applied Materials and Interfaces* 11.9 (Mar. 2019), pp. 9530–9538. ISSN: 19448252. DOI: 10.1021/ACSAMI.8B19433. URL: https://pubs.acs.org/doi/full/10.1021/acsami.8b19433.

[43] Timothy H. Bayburt and Stephen G. Sligar. "Membrane protein assembly into Nanodiscs". In: *FEBS letters* 584.9 (May 2010), pp. 1721–1727. ISSN: 1873-3468. DOI: 10.1016/J.FEBSLET.2009.10.024. URL: https://pubmed.ncbi.nlm.nih.gov/19836392/.

[44] Dongseok Moon, Yeon Kyung Cha, So ong Kim, et al. "FET-based nanobiosensors for the detection of smell and taste". In: *Science China. Life sciences* 63.8 (Aug. 2020), pp. 1159–1167. ISSN: 1869-1889. DOI: 10.1007/S11427-019-1571-8. URL: https://pubmed.ncbi.nlm.nih.gov/31974862/.

[45] Jamal Ahmed Cheema, Nihan Aydemir, Colm Carraher, et al. "Insect odorant receptor nanodiscs for sensitive and specific electrochemical detection of odorant compounds". In: *Sensors and Actuators, B: Chemical* 329 (Feb. 2021). ISSN: 09254005. DOI: 10.1016/J.SNB.2020.129243.

[46] Alexander Star, Jean Christophe P. Gabriel, Keith Bradley, et al. "Electronic detection of specific protein binding using nanotube FET devices". In: *Nano Letters* 3.4 (Apr. 2003), pp. 459–463. ISSN: 15306984. DOI: 10.1021/NL0340172. URL: https://pubs.acs.org/doi/full/10.1021/nl0340172.

[47] Jin Yoo, Daesan Kim, Heehong Yang, et al. "Olfactory receptor-based CNT-FET sensor for the detection of DMMP as a simulant of sarin". In: *Sensors and Actuators B: Chemical* 354 (Mar. 2022), p. 131188. ISSN: 0925-4005. DOI: 10.1016/J.SNB.2021.131188.

[48] Manki Son, Daesan Kim, Hwi Jin Ko, et al. "A portable and multiplexed bioelectronic sensor using human olfactory and taste receptors". In: 87 (Jan. 2017), pp. 901–907. DOI: 10.1016/J.BIOS.2016.09.040. URL: https://pubmed.ncbi.nlm.nih.gov/27664409/.

[49] By Tae Hyun Kim, Sang Hun Lee, Joohyung Lee, et al. "Single-Carbon-Atomic-Resolution Detection of Odorant Molecules using a Human Olfactory Receptor-based Bioelectronic Nose". In: *Advanced Materials* 21.1 (Jan. 2009), pp. 91–94. ISSN: 1521-4095. DOI: 10.1002/ADMA.200801435. URL: https://onlinelibrary.wiley.com/doi/full/10.1002/adma.200801435%20https://onlinelibrary.wiley.com/doi/abs/10.1002/adma.200801435%20https://onlinelibrary.wiley.com/doi/10.1002/adma.200801435.

[50] Juhun Park, Jong Hyun Lim, Hye Jun Jin, et al. "A bioelectronic sensor based on canine olfactory nanovesicle–carbon nanotube hybrid structures for the fast assessment of food quality". In: *Analyst* 137.14 (June 2012), pp. 3249–3254. ISSN: 1364-5528. DOI: 10.1039/C2AN16274A. URL: https://pubs.rsc.org/en/content/articlehtml/2012/an/c2an16274a%20https://pubs.rsc.org/en/content/articlelanding/2012/an/c2an16274a.

[51] Manki Son, Dong Guk Cho, Jong Hyun Lim, et al. "Real-time monitoring of geosmin and 2-methylisoborneol, representative odor compounds in water pollution using bioelectronic nose with human-like performance". In: 74 (Dec. 2015),

pp. 199–206. DOI: 10.1016/J.BIOS.2015.06.053. URL: https://pubmed.ncbi.nlm.nih.gov/26143459/.

[52] Jung Ho Ahn, Jong Hyun Lim, Juhun Park, et al. "Screening of target-specific olfactory receptor and development of olfactory biosensor for the assessment of fungal contamination in grain". In: *Sensors and Actuators B: Chemical* C.210 (2015), pp. 9–16. ISSN: 0925-4005. DOI: 10.1016/J.SNB.2014.12.060. URL: https://www.infona.pl//resource/bwmeta1.element.elsevier-a8cf00b4-326e-3e7c-87ab-72af38a2b71e.

[53] Minju Lee, Heehong Yang, Daesan Kim, et al. "Human-like smelling of a rose scent using an olfactory receptor nanodisc-based bioelectronic nose". In: 8.1 (2018), pp. 1–12. ISSN: 2045-2322. URL: https://www.nature.com/articles/s41598-018-32155-1%20https://pubmed.ncbi.nlm.nih.gov/30224633/.

[54] Nuriye Tuna Subasi. "Overview of Schiff Bases". In: *Schiff Base in Organic, Inorganic and Physical Chemistry* (Oct. 2022). DOI: 10.5772/INTECHOPEN.108178. URL: https://www.intechopen.com/chapters/84305%20undefined/chapters/84305.

[55] Dieter Wicher, Ronny Schäfer, René Bauernfeind, et al. "Drosophila odorant receptors are both ligand-gated and cyclic-nucleotide- activated cation channels". In: *Nature* 452.7190 (Apr. 2008), pp. 1007–1011. ISSN: 14764687. DOI: 10.1038/NATURE06861.

[56] Nathália F. Brito, Monica F. Moreira, and Ana C.A. Melo. "A look inside odorant-binding proteins in insect chemoreception". In: *Journal of Insect Physiology* 95 (Dec. 2016), pp. 51–65. ISSN: 0022-1910. DOI: 10.1016/J.JINSPHYS.2016.09.008.

[57] Peter J. Clyne, Coral G. Warr, Marc R. Freeman, et al. "A novel family of divergent seven-transmembrane proteins: candidate odorant receptors in Drosophila". In: *Neuron* 22.2 (1999), pp. 327–338. ISSN: 0896-6273. DOI: 10.1016/S0896-6273(00)81093-4. URL: https://pubmed.ncbi.nlm.nih.gov/10069338/.

[58] Dieter Wicher and Fabio Miazzi. "Functional properties of insect olfactory receptors: ionotropic receptors and odorant receptors". In: *Cell and Tissue Research* 383.1 (Jan. 2021), pp. 7–19. ISSN: 14320878. DOI: 10.1007/S00441-020-03363-X.

[59] Renee Smart, Aidan Kiely, Morgan Beale, et al. "Drosophila odorant receptors are novel seven transmembrane domain proteins that can signal independently of heterotrimeric G proteins". In: *Insect Biochemistry and Molecular Biology* 38.8 (Aug. 2008), pp. 770–780. ISSN: 09651748. DOI: 10.1016/J.IBMB.2008.05.002.

[60] Koji Sato, Maurizio Pellegrino, Takao Nakagawa, et al. "Insect olfactory receptors are heteromeric ligand-gated ion channels". In: *Nature* 452.7190 (Apr. 2008), pp. 1002–1006. ISSN: 14764687. DOI: 10.1038/NATURE06850.

[61] Colm Carraher, Julie Dalziel, Melissa D. Jordan, et al. "Towards an understanding of the structural basis for insect olfaction by odorant receptors". In: *Insect Biochemistry and Molecular Biology* 66 (Nov. 2015), pp. 31–41. ISSN: 18790240. DOI: 10.1016/J.IBMB.2015.09.010.

[62] Joel A. Butterwick, Josefina del Mármol, Kelly H. Kim, et al. "Cryo-EM structure of the insect olfactory receptor Orco". In: *Nature* 560.7719 (Aug. 2018), pp. 447–452. ISSN: 14764687. DOI: 10.1038/S41586-018-0420-8.

[63] Daniel Münch and C. Giovanni Galizia. "DoOR 2.0 - Comprehensive Mapping of Drosophila melanogaster Odorant Responses". In: *Scientific Reports* 6 (Feb. 2016). ISSN: 20452322. DOI: 10.1038/SREP21841. URL: /pmc/articles/PMC4766438/%20/pmc/articles/PMC4766438/?report=abstract%20https://www.ncbi.nlm.nih.gov/pmc/articles/PMC4766438/.

[64] Roshan Khadka, Nihan Aydemir, Colm Carraher, et al. "An ultrasensitive electrochemical impedance-based biosensor using insect odorant receptors to detect odorants". In: *Biosensors and Bioelectronics* 126 (Feb. 2019), pp. 207–213. ISSN: 0956-5663. DOI: 10.1016/J.BIOS.2018.10.043.

[65] Joana Galvao, Benjamin Davis, Mark Tilley, et al. "Unexpected low-dose toxicity of the universal solvent DMSO". In: *FASEB journal : official publication of the Federation of American Societies for Experimental Biology* 28.3 (2014), pp. 1317–1330. ISSN: 1530-6860. DOI: 10.1096/FJ.13-235440. URL: https://pubmed.ncbi.nlm.nih.gov/24327606/.

[66] K. Bradley, M. Briman, A. Star, et al. "Charge Transfer from Adsorbed Proteins". In: *Nano Letters* 4.2 (Feb. 2004), pp. 253–256. ISSN: 15306984. DOI: 10.1021/NL034985. URL: https://pubs.acs.org/doi/full/10.1021/nl0349855.

[67] Bajramshahe Shkodra, Mattia Petrelli, Martina Aurora Costa Angeli, et al. "Electrolyte-gated carbon nanotube field-effect transistor-based biosensors: Principles and applications". In: *Applied Physics Reviews* 8.4 (Dec. 2021), p. 41325. ISSN: 19319401. DOI: 10.1063/5.0058591. URL: /aip/apr/article/8/4/041325/1076095/Electrolyte-gated-carbon-nanotube-field-effect.

[68] Robert J. Chen, Hee Cheul Choi, Sarunya Bangsaruntip, et al. "An Investigation of the Mechanisms of Electronic Sensing of Protein Adsorption on Carbon Nanotube Devices". In: *Journal of the American Chemical Society* 126.5 (Feb. 2004), pp. 1563–1568. ISSN: 00027863. DOI: 10.1021/JA038702M. URL: https://pubs.acs.org/sharingguidelines.

[69] Basanta K. Das, Chaker Tlili, Sushmee Badhulika, et al. "Single-walled carbon nanotubes chemiresistor aptasensors for small molecules: Picomolar level detection of adenosine triphosphate". In: *Chemical Communications* 47.13 (Mar. 2011), pp. 3793–3795. ISSN: 1364548X. DOI: 10.1039/c0cc04733c. URL: https://pubs.rsc.org/en/content/articlehtml/2011/cc/c0cc04733c%20https://pubs.rsc.org/en/content/articlelanding/2011/cc/c0cc04733c.